

COMPARISON BETWEEN ONE- AND TWO-CHANNEL KONDO EFFECTS IN MESOSCOPIC SYSTEMS

A. Zawadowski

*Department of Theoretical Physics and Research Group of the Hungarian Academy of Sciences,
Technical University of Budapest, H-1521 Budapest, Hungary*

*Solid State and Optical Research Institute of the Hungarian Academy of Sciences, H-1525 Budapest,
Hungary*

There are strong recent indications that the Kondo phenomena play important role in the electronic transport and dephasing mechanism for some of the experimentally investigated metallic samples. The spin and the orbital Kondo problem with two-level systems provide very similar behavior above the Kondo temperature. Below the Kondo temperature the behavior is drastically different as in the latter case the entropy remains non zero. In the following several results derived earlier by different methods are simply reproduced by the time-ordered diagram technique in the leading logarithmic approximation valid above the Kondo temperature.

In the recent years the evidences have been fast growing that in many cases the low energy or low temperature electron transport in metals cannot be explained in terms of electron-electron and electron-phonon interactions. The anomalous behaviors occur e.g. in the electron dephasing rate¹ and mesoscopic transport^{2,3}. The leading candidates to resolve those problems are the Kondo phenomena due to dynamical impurities. The one-channel Kondo problem (1CK) is dealing with magnetic impurities, the two-channel one (2CK) may describe the interaction between the electrons and the fast relaxing two-level systems (TLS). In the 1CK problem the characteristic Kondo temperatures T_K cover a very broad temperature range, while in the 2CK case the zero bias anomalies indicate the typical range around $5K$ ³. In the second case the theoretical description of the Kondo temperature is still in debate^{4,5} but the electron-hole symmetry breaking in the electronic band structure seems to explain the observed value.

While the high temperature Kondo phenomena ($T > T_K$) are not very different in the 1CK and 2CK cases, in the low temperature range their behaviors are drastically different. Lowering the temperature the impurity dynamics is largely enhanced around T_K . In the 1CK the ground state is singlet, thus the dynamics is gradually frozen out and Fermi liquid behavior is developing as the zero temperature is approached. On the other hand the 2CK ground state without low energy cutoff (e.g. level splitting) has a finite entropy, thus the enhanced dynamics can exist even at very low temperature. In the 1CK case the electron dephasing rate goes to zero as $T \rightarrow 0$, for the 2CK case a new energy scale is suggested⁶, where the dephasing rate is slowly varying even well below the Kondo temperature. While the predictions are well confirmed for magnetic impurities, the role of TLS is still subject of intensive discussions which is partially due to the difficulties to identify the TLS-s in a real system. The non-universal behavior of dephasing rate at low temperature supports that in some cases the TLS may play a decisive role.

The recent experiments carried out by the Saclay group² in which the electronic transport in short wires is studied can be also very different for different metals, but also are very sensitive on impurities. The Ag and some of the Au samples show no anomalous behavior, closely following the predictions based on electron-electron interactions⁷. Some of the Au and the Cu samples show a fast electronic energy relaxation by smearing the electron distribution function around the Fermi energies corresponding to the left and right contacts. Recently, it became known that some of the Au samples contain fairly large amount of magnetic Fe impurities². The observed anomalies were explained in a phenomenological way by assuming an anomalous electron-electron scattering rate which is singular in the energy transfer E like $1/E^2$.

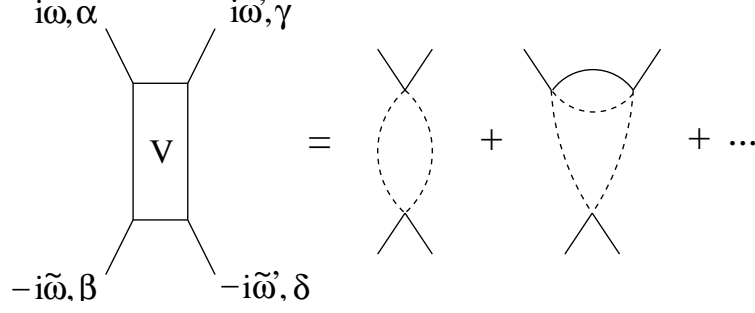


Figure 1: The effective magnetic impurity induced electron-electron interaction in the imaginary time technique. The diagrams contributing to lowest orders are also shown. The solid lines indicate the electrons, the dotted lines the Abrikosov's pseudofermions.

Such a behavior first derived by J. Kroha⁸ in the framework of the 2CK problem for $T < T_K$. Recently, it has been pointed out by Kaminski and Glazman^{9,10} that a similar behavior can be obtained for $T > T_K$ independently of the number of the channels. The result for $T < T_K$ in the 1CK case must be very different as in the framework of the Fermi liquid behavior no singular behavior can be expected.

The Kondo effect is due to the scattering of conduction electrons by a localized object (magnetic or substitutional impurity or some defects) with some internal degrees of freedom (e.g. spin, two close atomic positions). The typical Hamiltonian of Kondo-like problems is

$$H = \sum_{k\mu} \epsilon_k c_{k\mu}^\dagger c_{k\mu} + \sum_{\alpha} \epsilon_{\alpha} b_{\alpha}^{\dagger} b_{\alpha} + \sum_{k,k'} \sum_{\mu\nu\alpha\beta} V_{\mu\nu}^{\alpha\beta} c_{k\mu}^{\dagger} c_{k'\nu} b_{\alpha}^{\dagger} b_{\beta} \quad (1)$$

where ϵ_k is the electron kinetic energy with momentum k , $c_{k\mu}^{\dagger}$ creates an electron spherical wave with radial momentum k and internal quantum numbers μ and b_{α}^{\dagger} creates a heavy object with quantum number α (α being the spin, the position of the atom in the TLS, or a crystal field label of the impurity). Note that the internal indices μ and ν of the conduction electrons may also represent magnetic spin or orbital indices or a combination of these as well. $V_{\mu\nu}^{\alpha\beta}$ denotes the interaction coupling and a band cutoff D is applied.

That is obvious that a dynamical impurity with finite excitation energy can mediate energy transfer between the electrons as a localized phonon does. It was first pointed out in Ref.s¹¹ that magnetic impurities also mediate energy transfer even in the absence of external magnetic field and crystalline field splitting in third order of the exchange coupling, while the second order contributes to the elastic scattering¹². The result in the lowest orders of the perturbation for the electron-electron effective coupling for an electron pair of zero total energy ($\omega = \tilde{\omega}$) shown in Fig. 1 is

$$V_{\alpha\beta\gamma\delta}(\omega, \omega') = [V_{el}(\omega, \omega') + V_{inel}(\omega, \omega')] \sigma_{\alpha\gamma} \sigma_{\beta\delta}, \quad (2)$$

where the elastic and the inelastic parts are respectively

$$V_{el}(\omega, \omega') = \frac{1}{T} \frac{1}{3} S(S+1) J^2 \left[1 + 4J\rho_0 \ln \frac{D}{|\omega|} \right] \delta_{\omega\omega'} \quad (3)$$

and

$$V_{inel}(\omega, \omega') = \frac{1}{3} S(S+1) J^2 4(J\rho_0) \frac{\pi}{\omega - \omega'} (\text{sgn } \omega - \text{sgn } \omega'), \quad (4)$$

where T is the temperature and $i(\omega - \omega')$ is the energy transfer in which the inelastic part is singular. That vertex was used to calculate the correction to the superconducting temperature in the presence of magnetic impurities¹¹. In the analytic continuation to real energy variables these

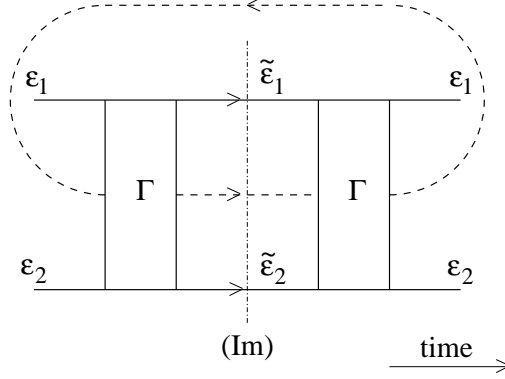


Figure 2: The two particle forward scattering amplitude $T(\omega)$ giving the decay rate is shown in time ordered representation, where the intermediate state providing the imaginary part is also shown.

contribute to the real part of the V_{inel} which is singular in the energy transfer E ($i(\omega - \omega') \rightarrow E$) as $1/E$.

Kaminski and Glazman⁹ were the first to point out that the magnetic impurity induced electron-electron scattering rate is also singular in the energy transfer. In the fourth order of the perturbation theory that was proportional to $1/E^2$, as the energy dependence assumed by the Saclay group².

In the following the derivation of that result with logarithmic correction is presented in the non-vanishing leading logarithmic order. The Abrikosov's pseudofermion technique¹³ is used, where the b operators in the Hamiltonian (1) create spin states and $V_{\mu\nu}^{\alpha\beta} \implies J\sigma_{\mu\nu}\mathbf{S}_{\alpha\beta}$ where J is the exchange coupling, σ is the Puli operator and \mathbf{S} is the spin operator describing the localized spin. For simplicity the time ordered diagrams are used with real time. That technique can be applied starting with arbitrary states (e.g. non-equilibrium) and the transition amplitude between states $|i\rangle$ and $\langle f|$ is given as

$$\langle f|T|i\rangle_{\omega} = \sum_{n=1}^{\infty} \langle f|H_1 \left(\frac{1}{\omega + i\delta - H_0} H_1 \right)^n |i\rangle, \quad (5)$$

where ω is the energy of the initial state. In the Abrikosov's pseudofermion technique¹³ the decay rate is calculated by taking the imaginary part of the forward scattering amplitude (using the optical theorem) thus

$$\frac{1}{\tau} \sim -\text{Im}\{\langle i|T|i\rangle_{\omega}\}. \quad (6)$$

In that diagram technique the pseudofermion lines representing the spin states (dotted line) are closed and there is only one line running against the time insuring that at any moment only one spin state is present for a given magnetic impurity. The electrons are represented by solid lines.

A typical forward scattering diagram which gives the result of Kaminski and Glazman, e.g. in the electron-electron channel⁹ in the leading logarithmic order is shown in Fig. 2, where the real part of vertex Γ is taken and the cut (dashed dotted line) represents the intermediate state where the imaginary part is taken. In the logarithmic approximation the vertex Γ is shown in Fig. 3, where the square boxes are parquet vertex correction $t(\tilde{\omega})$ with energy $\tilde{\omega}$ running through in the one particle channel and defined similarly to Eq. (5). The dotted line inside the one particle scattering amplitude runs in the direction of time.

Assuming that the total two-particle initial energy is ω and the energy transfer is e.g. $E = \varepsilon_1 - \tilde{\varepsilon}_1$, then the intermediate energy denominator e.g. in the diagram in Fig. 3 is $\omega - \tilde{\varepsilon}_1 - \varepsilon_2$, thus with $\omega = \varepsilon_1 + \varepsilon_2$ that is just the energy transfer. In this way the two-particle interaction rate is $\text{Im} T \sim \frac{1}{E^2}$.

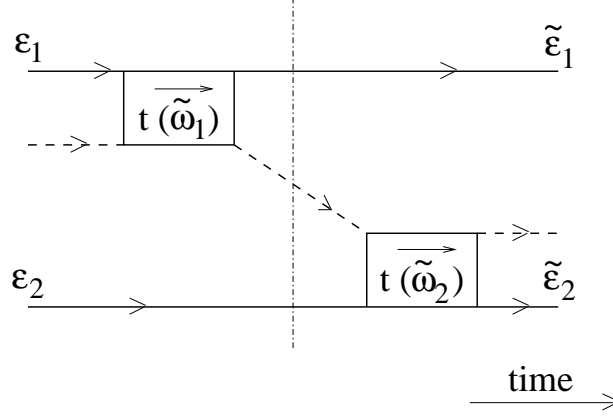


Figure 3: Typical time ordered diagram contributing to the vertex Γ in the leading logarithmic approximation is shown. The square boxes represent the electron-pseudofermion vertexes $t(\tilde{\omega})$ with total internal energy $\tilde{\omega}$. The dotted line represents the position of the energy denominator.

The one-electron scattering blocks $t(\tilde{\omega})$ are in logarithmic approximation ($|\tilde{\omega}| + kT > T_K$)

$$t(\tilde{\omega}) = \frac{J}{1 - 2J\rho_0 \ln \frac{D}{|\tilde{\omega}| + kT}} = \frac{1}{2\rho_0 \ln \frac{|\tilde{\omega}| + kT}{T_K}}. \quad (7)$$

where $T_K = D \exp\{-\frac{1}{2J\rho_0}\}$ is the Kondo temperature in the leading logarithmic approximation¹⁴. In the diagrams in Fig. 2 the one-particle vertex corrections represented by the square boxes are separated in time, thus their internal variables are $\tilde{\omega}_1 = \omega - \varepsilon_1$ and $\tilde{\omega}_2 = \omega - \tilde{\varepsilon}_1$, thus with $\omega = \varepsilon_1 + \varepsilon_2$, $\tilde{\omega}_1 = \varepsilon_1$ and $\tilde{\omega}_2 = \varepsilon_2 + E$. In this way the scattering rate is

$$\frac{1}{\tau(\omega)} \Big|_{\omega=\varepsilon_1+\varepsilon_2} \sim \frac{1}{E^2} \int (t(\varepsilon_1)t(\varepsilon_2 + E))^2 (1 - n(\tilde{\varepsilon}_1))(1 - n(\tilde{\varepsilon}_2)) \delta(\omega - \tilde{\varepsilon}_1 - \tilde{\varepsilon}_2) d\tilde{\varepsilon}_1 d\tilde{\varepsilon}_2, \quad (8)$$

where $n(\varepsilon)$ are the occupation numbers of the electronic states in the actual non-equilibrium states. There are similar other terms contributing to the right hand side of Eq. (8), where the vertex correction terms are of fourth order in the one-particle vertices ($t(\varepsilon_1)$, $t(\varepsilon_2)$, $t(\varepsilon_1 + E)$, $t(\varepsilon_2 - E)$) with different combinations. That result is identical with Eq. (10) in Ref.⁹ only the arguments of the vertex corrections are somewhat different. It is important to point out, that the vertex correction term cannot be factorized like $|\tau(\varepsilon_1)\tau(\varepsilon_2)|^2$ as it was suggested in Ref.¹⁰. See also Ref.¹⁵ where the slave boson technique is applied.

The vertex $t(\tilde{\omega})$ can be easily calculated even for the non-equilibrium case. Considering a short wire with bias V , the Fermi energy for the contact 1(2) is denoted by $E_{F_1}(E_{F_2})$, then $E_{F_2} - E_{F_1} = eV > 0$. Assuming that the distance of the impurity from contact 2 is pL where L is the length of the sample and $0 < p < 1$. Then the non-interacting distribution of the electrons at the impurity is represented by the heavy line in Fig. 4. The scattering amplitude $t(\tilde{\omega})$ can be calculated by poor man's scaling by eliminating electron and hole states above and below the energy $\tilde{\omega}$ in equal distances.

The elimination of states both occupied and unoccupied does not give logarithmic contribution thus they do not contribute to the scaling. The elimination is in two steps I and II. Take e.g. ω such that $E_{F_2} - \omega > \omega - E_{F_1}$, then in the first step I the electron-hole states are eliminated for which $n = 0$ or $n = 1$. In the step II only those electron states are eliminated which have unoccupied counter hole states and $n \neq 0$, $n \neq 1$, thus only portion p of the states. In the step II the initial coupling is the result obtained by step I. Thus

$$t^I(\tilde{\omega}) = \frac{J}{1 - 2J\rho_0 \ln \frac{D}{|E_{F_2} - \tilde{\omega}|}} \quad (9)$$

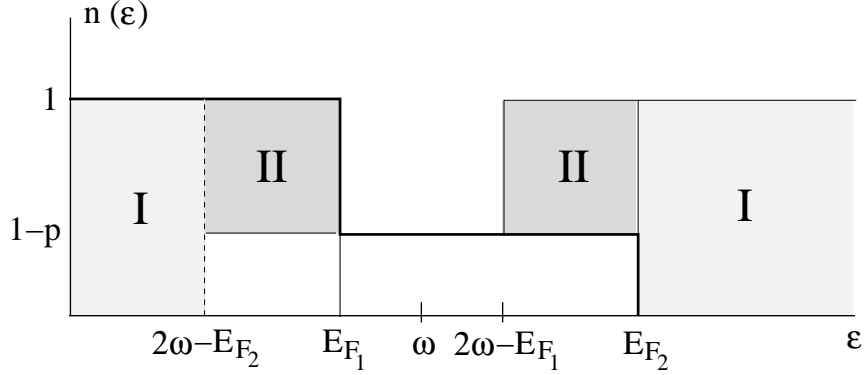


Figure 4: The electron distribution function in a wire at large bias eV is shown without the electron-electron interaction. The regions I and II are eliminated in the two steps, the heavy solid line separates the occupied and unoccupied regions.

and

$$t^{I+II}(\tilde{\omega}) = \frac{t^I(\tilde{\omega})}{1 - 2\rho_0 p t^I(E_{F_2} - \tilde{\omega}) \ln \frac{|E_{F_2} - \tilde{\omega}|}{\tilde{\omega} - E_{F_1}}}. \quad (10)$$

In Eq. (10) p occurs in the denominator. Here it is assumed that $|E_{F_2} - \tilde{\omega}| > \tilde{\omega} - E_{F_1} > T_K^0$, where T_K^0 is the bulk equilibrium Kondo temperature. In this case separate Kondo resonances are formed^{8,15} at the two Fermi energies E_{F_1} and E_{F_2} , and e.g. the width of the resonance described by the separate Kondo temperature T_K^1 is defined by $\tilde{\omega}$ where $t^{I+II}(\tilde{\omega}) \rightarrow \infty$. Thus

$$T_K^1 = \frac{(T_K^0)^{\frac{1}{p}}}{(eV)^{\frac{1}{p}-1}}. \quad (11)$$

That reproduces the result of Ref.¹⁶. T_K^2 can be obtained by electron-hole transformation and $p \rightarrow 1 - p$.

The inclusion of the Korringa type of spin life-time is beyond the leading logarithmic approximation¹⁷. In the case of large bias V the temperature is replaced by eV and that can play a dominating role which is not discussed here, but smears the $1/E^2$ singularity^{9,10,15}.

According to the experiments² the scaling in the distribution in the wire with a large bias holds only for the larger biases. Above the Kondo temperature $n(E/eV)$ depends on only one dimensionless variable as far as the Kondo corrections containing T_K^0 (or in an other form D) are negligible. Recently J. Kroha extended his slave boson calculation⁸ for $T > T_K$ and the entire problem is treated in Ref.¹⁵.

Acknowledgments

I express my gratitude to J. Kroha as the main part of the work has been carried out in collaboration with him and I borrowed many of his ideas. I am especially grateful among many others to H. Pothier, N.O. Birge, M. Devoret, B. Altshuler, L.I. Glazman, J. von Delft, O. Újsághy and G. Zaránd for useful discussions. This work was supported by Hungarian Grants OTKA T024005, T029813, T034243 and by the A. v. Humboldt foundation.

References

1. See e.g. P. Mohanty, E.M.Q. Jariwala and R.A. Webb, *Phys. Rev. Lett.* **78**, 3366 (1997).
2. H. Pothier, S. Guéron, Norman O. Birge, D. Esteve and M.H. Devoret, *Z. Phys. B* **104**, 178 (1997), *Phys. Rev. Lett.* **79**, 3490 (1997); F. Pierre, H. Pothier, D. Esteve, M.H. Devoret, A.B. Gougam and N.O. Birge, in *Proceedings of the NATO ARW "Size Dependent Magnetic Scattering", 28 May - 1 June 2000, Pécs, Hungary*, (Kluwer Academic, Dordrecht, 2000), cond-mat/0012038, and the present volume.
3. See for a recent review O. Újsághy, G. Zaránd and A. Zawadowski, *Solid State Commun.* **117**, 167 (2001).
4. I.L. Aleiner, B.L. Altshuler, Y.M. Galperin, T.A. Shutenko, *Phys. Rev. Lett.* **86**, 2629 (2001).
5. A. Zawadowski and G. Zaránd, cond-mat/0009283.
6. A. Zawadowski, J. von Delft and D. Ralph, *Phys. Rev. Lett.* **83**, 2632 (1999).
7. For a review, see B.L. Altshuler and A.G. Aronov, in *Electron-Electron interactions in Disordered Systems*, ed. A.L. Efros and M. Pollak, (Elsevier Science Publishers, B.V. 1985).
8. J. Kroha, *Adv. Solid State Phys.* **40**, 216 (2000).
9. A. Kaminski and L.I. Glazman, *Phys. Rev. Lett.* **86**, 2400 (2001).
10. See also Georg Göppert and Hermann Grabert, cond-mat/0102150.
11. J. Sólyom, A. Zawadowski, *Phys. Letters A* **25**, 91 (1967) and *Z. Physik* **226**, 116 (1969).
12. A.A. Abrikosov and L.P. Gorkov, *Zh. Eksperim. i. Theor. Fiz.* **39**, 1781 (1960), *Sov. Phys. JETP* **12**, 1243 (1961).
13. A.A. Abrikosov, *Physics* **2**, 5 (1965).
14. See e.g. G. Grüner, A. Zawadowski, *Reports on Progress in Physics* **37**, 1497 (1974).
15. J. Kroha and A. Zawadowski, cond-mat/0104151 and cond-mat/0105032.
16. P. Coleman, C. Hooley, O. Parcollet, *Phys. Rev. Lett.* **86**, 4088 (2001).
17. A. Zawadowski, P. Fazekas, *Z. Physik* **226**, 235 (1970).